SAND2013-10451C

Optimal Locations for Energy Storage Damping Systems in the Western North American Interconnect

R. H. Byrne[1], D. J. Trudnowski[2], J. C. Neely[1], R. T. Elliott[1], D. A. Schoenwald[1] and M. K. Donnelly[2]
[1]Sandia National Laboratories, PO Box 5800, Albuquerque, NM 87185–0576
[2]Montana Tech University, Electrical Engineering Department, Butte, MT 59701
Email:rhbyrne@sandia.gov

***Abstract*—Electromechanical oscillations often limit transmission capacity in the western North American Power System (termed the wNAPS). Recent research and development has focused on employing large-scale damping controls via wide-area feedback. Such an approach is made possible by the recent installation of a wide-area real-time measurement system based upon Phasor Measurement Unit (PMU) technology. One potential large-scale damping approach is based on energy storage devices. Such an approach has considerable promise for damping oscillations. This paper considers the placement of such devices within the wNAPS system. We explore combining energy storage devices with HVDC modulation of the Pacific DC Intertie (PDCI). We include eigenanalysis of a reduced-order wNAPS system, detailed analysis of a basic two-area dynamic system, and full-order transient simulations. We conclude that the optimal energy storage location is in the area with the lower inertia.**

Index Terms–Power system dynamics, stability, control, oscillations; HVDC modulation; energy storage.

I. Introduction

The western North American power system (wNAPS) consists of an interconnection of the entire western US and Canada and includes long transmission paths resulting in several modes of inter-area oscillation. These oscillations have historically been, and continue to be, a concern. For example, oscillatory instability was a contributing factor to the 1996 system break up [1]. Recent increased power transmission requests and observed low-damping events have spurred research and development activities to address oscillation damping. This includes implementation of a PMU-based real-time wide-area measurement system (WAMS) and the evaluation of large-scale oscillation damping devices that utilize WAMS feedback.

One control approach that has received considerable attention is modulation of the Pacific DC Intertie (PDCI) [2]. The PDCI is an 846-mile 3,100-MW DC transmission line connecting northern Oregon and southern California. It has extensive leverage on the electromechanical dynamics. The converter controls allow for modulation of the DC power on the line at a rate significantly above the bandwidth of the electromechanical dynamics. The approach in [2] modulates the DC power based upon the frequency error across the DC line. Using transient-stability and eigenanalysis model studies, it is demonstrated in [2] that this approach has significant advantages and performance.

A more generalized version of the PDCI approach is to symmetrically inject real power at the two ends of an oscillation based upon the frequency error between the two areas [3], [4]. The symmetrical injection can be achieved via HVDC modulation and/or energy storage. Other approaches investigated in [3], [4] include thyristor braking.

This paper expands the results in [2]-[4] by considering asymmetrical power injection. The goal is to minimize the amount of power modulation required to increase modal damping. We specifically focus upon the wNAPS system and the most troublesome north-south oscillations. We include eigenanalysis of a reduced-order wNAPS system, detailed analysis of a basic two-area dynamic system, and full-order transient simulations. We conclude that the optimal location for damping control systems is in the area with the smaller inertia.

II. Properties of the wNAPS

Inter-area mode properties of the wNAPS are discussed in more detail in [2]; the following is a summary. The inter-area modes of interest are:

- “NS Mode A” nominally near 0.25 Hz;
- “NS Mode B” nominally near 0.4 Hz;
- “BC” mode nominally near 0.6 Hz; and,
- “Montana” mode nominally near 0.8 Hz.

Other modes exist in the system; but, these four have been observed the most and are well understood. Of the four modes, NS Mode B is the most widespread and troublesome. It is the focus of this paper.

A. Mode Shape

NS Mode A has the northern half of the system (Canada and the pacific northwest US) swinging against the southern half (desert southwest US and southern California). By far, the dominant observability point of NS Mode A is in Alberta Canada. NS Mode B first showed up after Alberta interconnected to the system [5] and has a very widespread shape. It has the Alberta area swinging against British Columbia and the northern US which in turn swings against the southwest US. The mode dividing line is typically south of the California-Oregon intertie.

Historically, the Alberta interconnection has the strongest influence on NS Modes A and B. With Alberta connected, NS Mode B typically has the lowest damping and is the most widespread and troublesome. Its damping is influenced by flows from Canada to California, which are historically high during the summer season. With Alberta disconnected, NS Modes A and B meld into a single north-south mode nominally near 0.32 Hz which again has a dividing line near the COI. This mode is typically lightly damped.

B. Controllability

The current knowledge base for the controllability of the NS Modes A and B is primarily based upon model studies. One approach employed to study the controllability is a reduced-order model of the system presented in [2]. This system is shown in Figure 1.

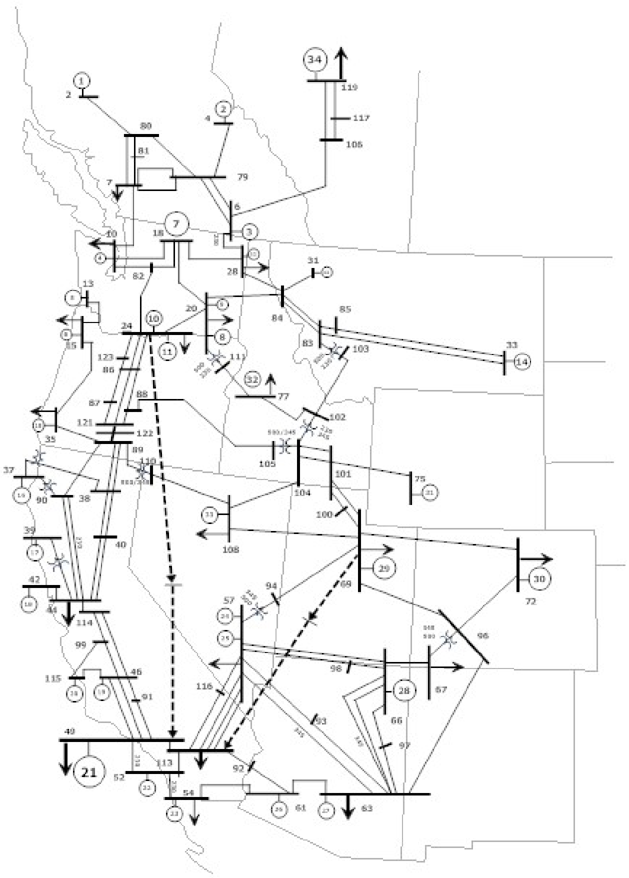

Fig. 1. One-line of wNAPS reduced-order model.

One perspective on controllability is the open-loop transfer function residue. The residue is an excellent measure of controllability. It represents the vector of departure in the root locus [6]. Ideally, the magnitude is large and the angle is near $\pm 180°$. This indicates the root locus is traveling to the left.

Table I shows the normalized open-loop transfer-function residues for NS Mode B for two different power-flow cases. Power-flow case 1 has generator 34 (Alberta) connected while power-flow case 2 has generator 34 disconnected. The "Bus 18" row is for power injection at bus 18 and an output of the relative speed between generators 7 and 23. The "Bus 54" row is for power injection at bus 54 and an output of the relative speed between generators 23 and 7. Because the residue magnitude at bus 18 is nearly double that for bus 54, one can conclude that real-power modulation control at bus 18 will likely have double the increased damping for a given modulation gain. Simulation results in [3], [4] verify this. The following two-mass system attempts to correlate the larger controllability with the inertia in each area.

TABLE I
OPEN-LOOP TRANSFER-FUNCTION RESIDUES.

	Case 1		**Case 2**	
Input	$\|R\|$	$\angle$ (deg)	$\|R\|$	$\angle$ (deg)
Bus 18	0.585	-178	0.58	-175
Bus 54	0.218	155	0.31	157

III. Control Strategy

Our control strategy is to derive a feedback signal that will proportionally provide damping to all modes when used to modulate real-power injection, and that won't interact with speed governor actions. Because we assume real-time access to a WAMS, we have the ability to derive this idealistic feedback.

When analyzing power systems, it is well known that one can improve damping by feeding back generator speed as a torque (termed damping torque) [7]. This concept is expanded in [8] to the modulation of real power in two areas based upon the relative frequency between two areas. The concept is relatively simple. Real power is injected into the system in two areas proportional to the frequency difference between the two injection points. Ideally, the injection points are on the two ends of an oscillation. This concept is the basis for what follows.

Given a two-area system shown in Figure 2, the control law at each damping control node is given by

$$\Delta P_{D1} = -K(f_1(t) - f_2(t-\tau)) \tag{1}$$

$$\Delta P_{D2} = -K(f_2(t) - f_1(t-\tau)) \tag{2}$$

where ΔP_{Di} is the real power injected at node i, f_i is the frequency measurement at node i, and τ is the message transport delay for the distant frequency measurement. The controller gain at each node is the same, resulting in a symmetric control response at each node. An example of this approach would be modulation of the Pacific DC Intertie. Neglecting losses, the power injected at one end is approximately the power received at the other end.

If energy storage or other real power injection techniques are to be employed in conjunction with PDCI modulation, the actuation signals will no longer be symmetric. An example would be co-locating an energy storage based damping control system at one end of the PDCI. To analyze the behavior of such a system, the simplified two-area linear system model shown in Figure 3 illustrates the basic system dynamics [9]. The model parameters are summarized in Table II.

The two-area model simplifies to the following state space system.

$$\dot{\boldsymbol{x}} = A\boldsymbol{x} + B\boldsymbol{u} \tag{3}$$

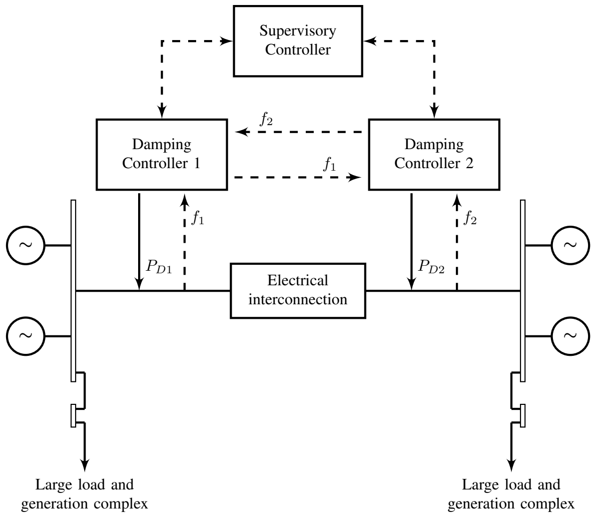

Fig. 2. Two-area system with damping control.

TABLE II
TWO-AREA SYSTEM MODEL QUANTITIES

Quantity	Description
M_i	Area i inertia
D_i	Area i damping
T	Synchronizing torque coefficient
ΔP_{Li}	Area i load variation
ΔP_{Di}	Area i damping torque
$\Delta \omega_i$	Area i change in speed
$\Delta \delta_i$	Area i change in angle

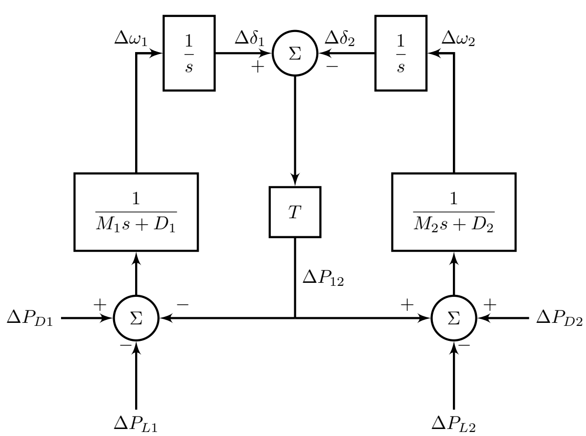

Fig. 3. Two-area system [9] with damping control.

where

$$\boldsymbol{x} = \begin{bmatrix} \Delta\omega_1 \\ \Delta\delta_1 \\ \Delta\omega_2 \\ \Delta\delta_2 \end{bmatrix} \quad (4)$$

$$A = \begin{bmatrix} -\frac{D_1}{M_1} & -\frac{T}{M_1} & 0 & \frac{T}{M_1} \\ 1 & 0 & 0 & 0 \\ 0 & \frac{T}{M_2} & -\frac{D_2}{M_2} & -\frac{T}{M_2} \\ 0 & 0 & 1 & 0 \end{bmatrix} \quad (5)$$

$$B = \begin{bmatrix} \frac{1}{M_1} & 0 \\ 0 & 0 \\ 0 & \frac{1}{M_2} \\ 0 & 0 \end{bmatrix}, \quad \boldsymbol{u} = \begin{bmatrix} \Delta P_{D1} \\ \Delta P_{D2} \end{bmatrix} \quad (6)$$

In order to accommodate an asymmetric controller, the control laws in equations (1)-(2) are redefined in terms of a scale factor $\alpha \in [0, 1]$,

$$\Delta P_{D1} = -K\alpha(f_1(t) - f_2(t - \tau)) \quad (7)$$

$$\Delta P_{D2} = -K(1 - \alpha)(f_2(t) - f_1(t - \tau)) \quad (8)$$

Assuming that the communication delays are negligible, the dynamics of the closed-loop system are captured by

$$A_{CL} = \begin{bmatrix} -\frac{D_1 + K\alpha}{M_1} & -\frac{T}{M_1} & \frac{K\alpha}{M_1} & \frac{T}{M_1} \\ 1 & 0 & 0 & 0 \\ \frac{K(1-\alpha)}{M_2} & \frac{T}{M_2} & -\frac{D_2 + K(1-\alpha)}{M_2} & -\frac{T}{M_2} \\ 0 & 0 & 1 & 0 \end{bmatrix} \quad (9)$$

Solving for the characteristic polynomial of the closed-loop system yields

$$p(s) = as^4 + bs^3 + cs^2 + ds + e \quad (10)$$

where

$$a = M_1 M_2 \quad (11)$$
$$b = M_1 D_2 + M_2 D_1 + M_1 K(1 - \alpha) + M_2 K\alpha \quad (12)$$
$$c = T(M_1 + M_2) + D_1 D_2 + D_1 K(1 - \alpha) + D_2 K\alpha \quad (13)$$
$$d = T(D_1 + D_2) \quad (14)$$
$$e = 0 \quad (15)$$

One pole is at the origin, leaving a 3^{rd} order polynomial. We are interested in the roots of this polynomial for the case of one real root and two complex conjugate roots. It should be noted that by inspection, if the area damping D_i and inertias M_i are equal, the characteristic polynomial is no longer a function of α. For this case the location of the damping controller does not affect damping performance.

For a third order polynomial, it is possible to factor out the real root p_1 using the Ruffini-Horner method [10].

$$p(s) = as^3 + bs^2 + cs + d \quad (16)$$

$$p(s) = (s - p_1)\left(s^2 + s(\frac{b}{a} + p_1) + \frac{c}{a} + \frac{b}{a}p_1 + p_1^2\right) \quad (17)$$

The real part of the complex pole (e.g. rate of decay) and the natural frequency are given by

$$\zeta\omega_n = \frac{1}{2}\left(\frac{b}{a} + p_1\right) \quad (18)$$

$$\omega_n^2 = \left(\frac{c}{a} + \frac{b}{a}p_1 + p_1^2\right) \quad (19)$$

Singular perturbation theory may be applied to arrive at an approximation for the real pole p_1 [11]. For a large T, e.g. a tightly coupled system, the characteristic polynomial may be approximated as

$$p(s) \approx s\,(cs + d) \quad (20)$$

Solving for the non-zero pole yields

$$p_1 \approx \frac{-T(D_1+D_2)}{T(M_1+M_2)+D_1D_2+D_1K(1-\alpha)+D_2K\alpha} \quad (21)$$

For large T, this further reduces to

$$p_1 \approx -\frac{D_1+D_2}{M_1+M_2} \quad (22)$$

Using this approximation (accurate to $\sim 1\%$ for typical values of M and D), equation (18) may be rewritten as

$$\zeta\omega_n \approx \frac{1}{2}\left(\frac{D_2}{M_2}+\frac{D_1}{M_1}+\frac{K(1-\alpha)}{M_2}+\frac{K\alpha}{M_1}-\frac{D_1+D_2}{M_1+M_2}\right) \quad (23)$$

It is clear that the rate of decay is maximized when α is selected such that all of the damping actuation is in the area with the lower inertia. The next section looks at the eigenvalues of the closed-loop system as α varies between 0 and 1 for the case of $M_2 = 2M_1$ using typical parameters. The movement of the closed-loop eigenvalues is easily visualized graphically given a set of system parameters.

IV. Eigenvalues of the Two-Area Closed-Loop System

In order to illustrate the optimal asymmetric gain which provides maximum damping, a two-area system with unequal inertias was analyzed. The model parameters are listed in Table III. The trajectory of the closed-loop eigenvalues, as α is varied between 0 and 1, is shown in Figure 4. The red 'o' indicates $\alpha = 0$ while the blue 'x' indicates $\alpha = 1$. With unequal inertias, the parameter α has an affect on the damping of the closed-loop eigenvalues. The maximum damping is obtained when $\alpha = 1$, which corresponds to placing all of the control actuation in the area with the smaller system inertia. This is intuitive and consistent with equation (23). For two areas oscillating against each other, applying control effort to the area with less inertia will have the most affect in damping out the inter-area oscillations. The next section evaluates several different control scenarios using the Western Electricity Coordinating Council (WECC) 2013 heavy summer PSLF (Positive Sequence Load Flow Software from General Electric) base case to show that this same phenomenon is present in large power systems.

TABLE III
Model parameters for simplified two-area system

Parameter	Value
M_1	4 sec
M_2	8 sec
D_1	1.2
D_1	1.2
T	3.132
K	0.3

V. Eigenvalues of WECC 2013 Heavy Summer PSLF Base Case

A WECC 2013 heavy summer PSLF base case (13hs_146a01.sav) developed by the Bonneville Power Adminstration was employed to illustrate the impact of

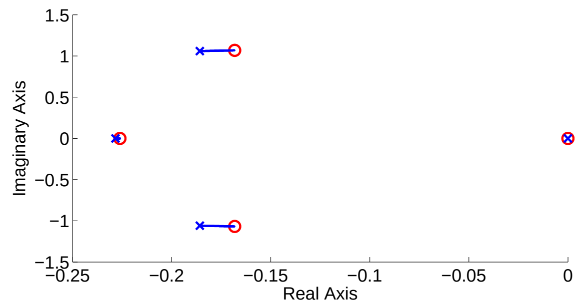

Fig. 4. Closed-loop eigenvalues as α varies from 0 to 1 ($M_2 = 2M_1$). The red 'o' indicates $\alpha = 0$ while the blue 'x' indicates $\alpha = 1$.

energy storage location on damping control performance. Based on the analysis of the simplified model for a two-area system, one would expect an energy storage damping control system to have the most impact located in the area with the smaller inertia. PDCI modulation has the greatest impact on the NS mode B. Therefore, this analysis will focus on this eigenvalue. In order to assess the inertias of various regions, a PSLF epcl program was written to calculate the inertia of all generators and loads modeled as rotating machines by WECC area.

$$J = \frac{2H(\text{MVA base})}{\omega_o^2}, \quad kg \cdot m^2 \quad (24)$$

where H is the inertia constant in seconds, w_0 is the generator angular velocity, and MVA base is the generator rating [12].

The results for the 2013 heavy summer base case are summarized in Table IV. Each region was classified as 'northern' or 'southern' based on its geographic location. For this particular base case, the inertia of the pacific northwest is significantly less than the inertia of the southwest. This is a rough estimate of the relative inertias of the two regions that participate in the NS mode B. A more accurate approach would be to determine the generators/loads that participate in the mode and sum the inertias from the two sets that oscillate against each other. A rough estimate is suitable for this analysis since the end goal is to simply demonstrate that the location of an energy storage damping system that augments PDCI modulation is important.

TABLE IV
2013 WECC heavy summer base case, inertia by WECC area ($kg \cdot m^2$). Northern areas are indicated by 'N' while southern areas are indicated by 'S'. Total southern inertia is 6,397,841 while the total northern inertia is 3,355,033.

WECC area	gen inertia	load inertia	total inertia	N/S
Arizona	1750185.38	10070.08	1760255.45	S
Mexico-CFE	153512.25	0.00	153512.25	S
Imperial CA	104790.92	0.00	104790.92	S
San Diego	264102.41	0.00	264102.41	S
So. Calif.	1608605.88	26175.96	1634781.83	S
LADWP	336956.59	22556.97	359513.57	S
PG & E	2095445.50	25439.47	2120884.97	S
Northwest	1843026.75	3638.56	1846665.31	N
B.C. Hydro	792542.63	24291.40	816834.03	N
Fortis B.C.	35133.55	4969.22	40102.77	N
Alberta	597615.94	53815.44	651431.38	N

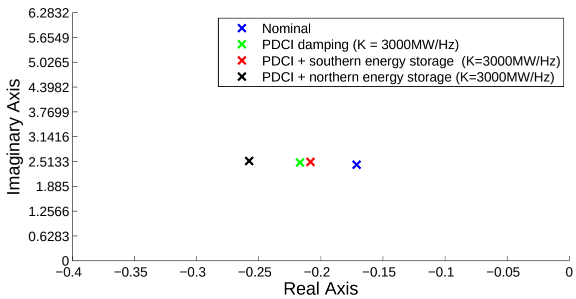

Fig. 5. WECC 2013 heavy summer base case eigenvalue location for the NS mode B.

Four different scenarios were simulated to illustrate the impact of energy storage damping controller location:

- Nominal base case with no damping control.
- PDCI modulation ($K = 3000$ MW/Hz).
- PDCI modulation plus energy storage system located at the south end ($K = 3000$ MW/Hz).
- PDCI modulation plus energy storage system located at the north end ($K = 3000$ MW/Hz).

A Chief Joseph brake insertion for 0.5 seconds was used to stimulate the system. The Eigensystem Realization Algorithm (ERA) was applied to generator speeds to identify the eigenvalue location of the NS mode B for each scenario. The ERA algorithm is described in [13] and power system applications are presented in [14], [15], [16]. The results are summarized in Figure 5. All three active control scenarios resulted in improved damping of the NS mode B. However, the controller located at the north end of the PDCI provided the most damping. This was consistent with the inertia estimate by area and the results for a two-area system.

VI. Conclusion

Real power modulation via WAMS feedback has been identified as a promising approach for damping inter-area oscillations in the wNAPS. Previous research has developed a symmetric control system based on PDCI real power modulation for damping the NS mode B. This paper builds on the symmetric controller design by exploring the performance of an asymmetric controller, e.g. PDCI modulation augmented with energy storage. A simplified two-area system model was used to show the behavior of the closed-loop eigenvalues as the symmetry of the control law was varied. For a two-area system with equal inertias, the location of the damping controller does not impact the location of the closed-loop eigenvalues. However, for the case with asymmetric inertias, the “optimal” controller location for the maximum damping is in the area with the lower inertia. This is intuitive, as it is easier to ‘move’ the area with the lower inertia given the same control effort.

Four different scenarios were then considered with a model of the wNAPS using the WECC 2013 heavy summer PSLF base case. These results were consistent with the eigenvalues derived for the simplified two-area system. Augmenting PDCI modulation with an energy storage device located in the region with the smaller inertia has the biggest impact on improving damping of the NS mode B. This behavior was also observed in a reduced-order model of the WECC. Future research will focus on damping multiple inter-area modes by augmenting PDCI modulation with energy storage.

Acknowledgment

The authors would like to thank the Department of Energy (DOE) Energy Storage Program (Dr. Imre Gyuk), the DOE Transmission Reliability Program (Mr. Phil Overholt), and the Bonneville Power Administration Technology Innovation Program (Dr. Jisun Kim and Dr. Dmitry Kosterev) for funding this research. Sandia National Laboratories is a multi-program laboratory managed and operated by Sandia Corporation, a wholly owned subsidiary of Lockheed Martin Corporation, for the U.S. Department of Energys National Nuclear Security Administration under contract DE-AC04-94AL85000.

References

[1] D. N. Kosterev, C. Taylor, and W. Mittelstadt, “Model validation for the August 10, 1996 WSCC system outage,” *IEEE Transactions on Power Systems*, vol. 14, no. 3, pp. 967–979, 1999.

[2] D. J. Trudnowski, D. Kosterev, and J. Undrill, “PDCI damping control analysis for the western north american power system,” in *Proceedings of the 2013 IEEE Power and Energy Society General Meeting*, Vancouver, B.C., July 2013.

[3] J. Undrill and D. J. Trudnowksi, “Oscillation damping controls,” Report to Bonneville Power Administration, contract 37508, Portland, OR, Tech. Rep., September 2008.

[4] J. Undrill, “Investigation of asymptotic stability of low frequency oscillations,” Report to Bonneville Power Administration, contract 37508, Portland, OR, Tech. Rep., September 2010.

[5] R. L. Cresap and J. Hauer, “Emergence of a new swing mode in the western power system,” *IEEE Transactions on Power Apparatus and Systems*, vol. PAS-100, no. 4, pp. 2037–2045, 1981.

[6] F. Pagola, I. Perez-Arriaga, and G. C. Verghese, “On sensitivities, residues and participations: applications to oscillatory stability analysis and control,” *IEEE Transactions on Power Systems*, vol. 4, no. 1, pp. 278–285, 1989.

[7] G. Rogers, *Power System Oscillations*. Boston: Kluwer Academic Publishers, 2000.

[8] J. Undrill, “Oscillation damping controls, Appendix 1, power system oscillations: Concepts and methods of control,” Report to Bonneville Power Administration, contract 37508, Portland, OR, Tech. Rep., September 2008.

[9] P. Kundur, *Power System Stability and Control*. New York: McGraw-Hill, Inc., 1993.

[10] M. W. Baldoni, C. Ciliberto, and G. M. P. Cattaneo, *Elementary Number Theory, Cryptography, and Codes*. Berlin: Springer-Verlag, 2009.

[11] M. H. Holmes, *Introduction to Perturbation Methods*. New York: Springer, 1995.

[12] P. Krause, O. Wasynczuk, and S. D. Sudhoff, *Analysis of Electric Machinery and Drive Systems*, 2^{nd} ed. Piscataway, NJ: IEEE Press and Wiley-InterScience, 2002.

[13] J.-N. Juang and R. S. Pappa, “An eigensystem realization algorithm for modal parameter identification and model reduction,” *AIAA Journal of Guidance,Control, and Dynamics*, vol. 8, no. 5, pp. 620–627, September 1985.

[14] J. J. Sanchez-Gasca and J. H. Chow, “Performance comparison of three identification methods for the analysis of electromechanical oscillations,” *IEEE Transactions of Power Systems*, vol. 14, no. 3, pp. 995–1002, 1999.

[15] J. J. Sanchez-Gasca, “Identification of power system low order linear models using the ERA/OBS method,” in *Proceedings of the 2004 IEEE PES Power Systems Conference and Exposition*, vol. 1, 2004, pp. 392–397.

[16] J. J. Sanchez-Gasca and J. H. Chow, “Computation of power system low-order models from time domain simulations using a hankel matrix,” *IEEE Transactions on Power Systems*, vol. 12, no. 4, pp. 1461–1467, 1997.